Secondary Arc Duration on a 380-kV Mixed Transmission Line during SPAR

Mustafa Kizilcay, Marcin Bozek, Nils Pfeifer

***Abstract*-- The transmission system expansion plan of Germany foresees several new EHV (Extra High Voltage) transmission lines to transmit bulk power generated by wind farms in the north of Germany to the South. Some of these EHV lines will be so called "mixed lines" consisting of several underground cable and overhead line sections. The high charging current of XLPE cables has to be compensated by shunt reactors. A planned double-circuit 380-kV transmission line with total length of ca. 110 km is of interest for the analysis of SPAR (single-phase autoreclosure) operation in this paper, where a cable section along the line has a length of 5.5 km. By means of electromagnetic transients simulations the maximum secondary arc duration will be determined for the mixed line under various operating conditions.**

***Keywords*: secondary arc, single-phase autoreclosure, SPAR, EHV mixed line.**

I. Introduction

THE generation capacity of wind farms in the north and northeastern area of Germany has significantly increased during the last ten years. This tendency will continue and even increase. The phasing out of nuclear power in Germany leads to the shutdown of power plants mainly in the southern part of Germany and causes a regional deficit of generation capacity. As a consequence, the German transmission grid needs significant reinforcements for the integration of renewable energy into the power system as well as to ensure the security of supply in the South. With the rising public concern regarding erection of new overhead transmission lines, the installation of EHV underground cable sections has become important. Consequently a part of the planned 380-kV transmission lines will be realized as so called "mixed transmission lines". Mixed transmission lines consist of both overhead line (OHL) sections and several underground XLPE cable sections [1], [9]. To compensate for the high capacitive charging current of XLPE cable sections shunt reactors are required. Either they will be installed in the cable transfer stations (CTS) along the line or in the substations (S/S) at both ends of the line. In the first case they will be switched on/off together with the complete transmission line. In the second alternative the shunt reactors are switched independently from the line. That choice of shunt compensation has an effect also on the secondary arc behavior during single-phase autoreclosure (SPAR).

This paper presents electromagnetic transients (EMT) study results to identify the maximum duration of the secondary arc, i.e. dead time as worst case in case of SPAR based on a planned 380-kV double-circuit mixed line with a total length of 112 km including a 5.5 km underground cable section. For that purpose various operating conditions of the line like line current, voltage, fault location along the line are taken into consideration.

The paper is structured as follows: System data and models of the components are described in Section II. Results of the simulations for various operating conditions are presented and discussed in Section III. Finally, important conclusions are summarized in Section IV.

II. System Data and Simulation Model

The configuration of the studied 380-kV transmission line is shown in Fig. 1. The double-circuit line consists of two OHL and one underground cable sections. The capacitive charging current of the transmission line will be compensated by maximum four shunt reactors each with a rated power of 120 MVAr connected to the busbars in the substations (S/S) A and D as shown in Fig. 1. The cable section (5.5 km) is located between the CTS B and C. The total capacitive reactive power of one circuit amounts to 194 MVAr at 400-kV voltage level.

Along the OHL sections there are several parallel 110-kV OHL sections of ca. 57 km total length for the railway power supply with $f = 16⅔$ Hz and one 110-kV, 50-Hz, OHL section of 11 km length on the same tower as the 380-kV OHL. Those OHL lines at the 110-kV level are transposed in addition to the

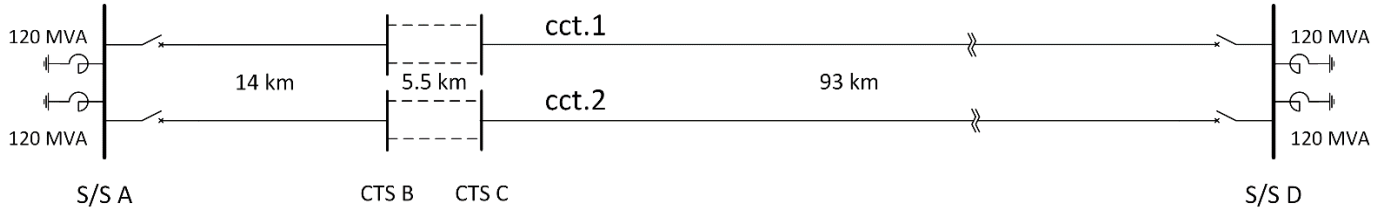

Fig. 1. Configuration of the 380-kV double-circuit mixed line with OHL (——) and cable (- - -) sections

M. Kizilcay and N. Pfeifer are with the Dept. ETI, University of Siegen, D-57068 Siegen, Germany (e-mail of corresponding author: kizilcay@uni-siegen.de, nils.pfeifer@uni-siegen.de). M. Bozek is with the Dept. Asset Management, TenneT TSO GmbH, D-95448 Bayreuth, Germany (e-mail: marcin.bozek@tennet.eu).

Paper submitted to the International Conference on Power Systems Transients (IPST2023) in Thessaloniki, Greece, June 12-15, 2023.

transpositions of the 380-kV line. Those parallel circuits and transpositions are not indicated Fig. 1 for the sake of simplicity.

A. Source Network Equivalents

The 380-kV grid connected in S/S A and D (Fig. 1) is represented by a simplified Thevenin equivalent using available positive- and zero-sequence short-circuit impedances given in Table I. The line-to-line voltage behind the three-phase short-circuit impedance is selected as 420 kV (max. operating voltage).

TABLE I
SHORT-CIRCUIT IMPEDANCES TO REPRESENT NETWORK EQUIVALENTS AND EQUIVALENT SERIES BRANCH BETWEEN SUBSTATIONS

	Pos.-sequence impedance Z_1 (Ω)		Zero-sequence impedance Z_0 (Ω)		Equiv. series branch S/S A – S/S D	
	S/S A	S/S D	S/S A	S/S D	Z_1 (Ω)	Z_0 (Ω)
For max. SC current	1.039 + j16.408	0.570 + j5.525	3.075 + j33.656	2.014 + j16.495	18.24 + j123.02	1958.28 + j4670.6
For min. SC current	2.903 + j28.037	1.383 + j8.883	10.115 + j68.121	3.595 + j24.744	66.32 + j259.85	5349.64 + j9782.2

B. Overhead Line Data

As it has been described above, 110-kV lines (2-phase OHL's for railway power supply and 3-phase OHL's) are carried on the towers for 380-kV OHL in certain line sections. The typical tower layout of those lines is shown in Fig. 2.

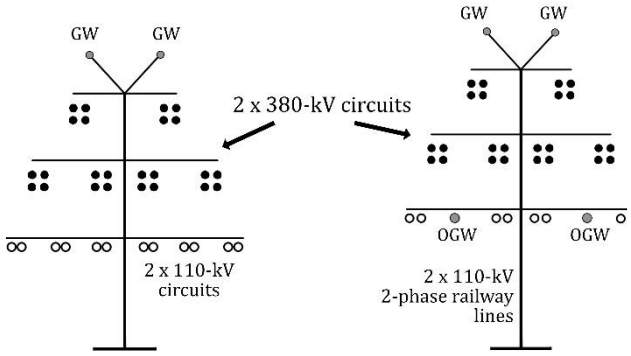

Fig. 2. Tower layout of the multi-circuit lines with 380-kV and 110-kV OHL's (GW: ground wire; OGW: optical ground wire)

The 380-kV circuits consist of 4-bundle conductors, whereas 110-kV lines are constructed using 2-bundle conductors. In addition, along the OHL route there is a line section of length 4.6 km in the long part of the OHL section (not shown in Fig. 1), where four 380-kV circuits are on the same tower, from which two circuits belong to another external 380-kV line. The conductor types of lines are given in TABLE II.

TABLE II
TYPES OF PHASE CONDUCTORS AND GROUND WIRES OF THE OVERHEAD LINES

Voltage level	Phase conductors	Ground wires / optical ground wires
380 kV	4 x 565/72 ACSR	304/49 ACSR / 261/25 ACSR
110 kV 3-phase line	2 x 264/34 ACSR	
110 kV 2-phase railway line	2 x 304/49 ACSR 2 x 264/34 ACSR	

The electrical parameters of one circuit of the OHL are as follows (assumed as ideally transposed):

$Z_{pos} = (0.0133 + 0.235i)\,\Omega/\text{km};\ Z_{zero} = (0.113 + 0.902i)\,\Omega/\text{km}$

$C_{pos} = 15.11\,\text{nF/km};\quad C_{zero} = 6.5\,\text{nF/km}.$

The multi-circuit OHL sections are represented by "Constant-Parameter Distributed Line (CPDL)" model, whereas the cable section divided in cross-bonding sections is modelled by multi-conductor Pi circuits [2], [3].

C. Cable Section

The 380-kV underground cable section is located near to S/S A as shown in Fig. 1. There is a need of two XLPE cables per phase to transport the same power of one circuit of the 380-kV OHL. Thus total 12 cables are installed for the double-circuit 380-kV OHL. The type of the cable is 2XS(FL)2Y 1x2500 RMS/250. Fig. 3 shows three single-core cables and cross-bonding of the cable sheaths that are protected by surge arresters. There are additional three cables belonging to the same circuit of the 380-kV OHL, which are not shown in this figure because of complexity. Cable sheaths are grounded only at one end of the cable section.

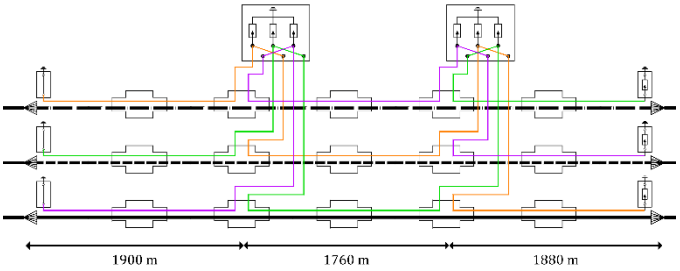

Fig. 3. Three single-core cables with cross-bonded cable sheaths at two joints

The single-core cables were laid in protecting plastic pipes in a depth of 1.6 m in a flat arrangement as shown in Fig. 4 [1]. In this particular study it is not necessary to model the sheath surge arresters. Their effect is negligible with regard to the secondary arc performance. The capacitance of one single-core cable computed using CABLE PARAMETERS [2] is 203 nF/km compared to the measured value of 219 nF/km by the manufacturer. For the cable model, the equivalent relative dielectric constant of the XLPE insulation is determined by taking the inner and outer semi-conductive layers into consideration [12]. Taking also the capacitances of the OHL line sections into account, the resulting capacitive reactive power amounts to 194 MVAr for one 380-kV circuit.

D. Shunt Reactors

The location of the 420-kV iron-core shunt reactors (SR) as a three-phase unit in wye-connection is shown in Fig. 1. The neutral point is grounded solidly. The design parameters are as follows:

- rated power: 120 MVA; rated voltage: 420 kV
- total losses: 170 kW.

Shunt reactors are modelled in a simplified form as a linear component using the equivalent circuit shown in Fig. 5. The ratio of the iron-core losses to the copper losses is assumed to be 0.6 based on measurements of a similar shunt reactor.

Since the shunt reactors are installed in the S/S A and S/S D, they will have no direct interaction with the secondary arc during SPAR.

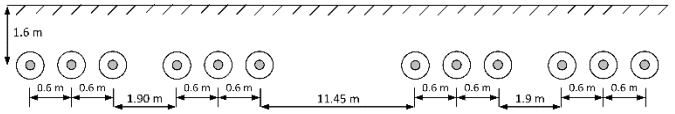

Fig. 4. Layout of 12 underground cables of the cable section

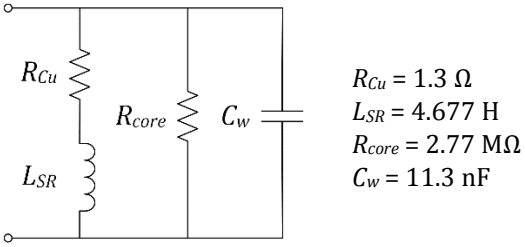

Fig. 5. Equivalent circuit of one phase of the shunt reactor

E. Fault Arc Model

During SPAR of the faulted circuit extinction behavior of secondary arc should be investigated. Primary arc is effective after fault inception until single-phase tripping of the faulty phase. Secondary arc follows the primary arc after isolating the fault by single phase disconnection at both ends. The transient interaction of the arc with the shunt compensated line can be investigated by a dynamic arc model [4] – [7].

The arc model used in this work is based on the energy balance of the arc column and describes an arc in air by a differential equation of the arc conductance g [4], [7]:

$$\frac{dg}{dt} = \frac{1}{\tau}\left(G - g\right) \tag{1}$$

where

τ : arc time constant,
g : instantaneous arc conductance,
G : stationary arc conductance.

Derivation of these parameters depending on voltage level and clearance over insulators – is equivalent to initial arc length – and details of the arc modelling in EMTP-ATP are provided in [7]. The length of the primary arc is considered to be constant. A linear time-varying elongation of the secondary arc is taken into account by the model. In reality the arc length variation is highly dependent on external factors like wind, thermal buoyancy. The arc time constant τ is assumed to be constant during the primary arc. The time constant of the secondary arc is time-varying and is expressed as a function of arc elongation with the parameter $\alpha = -0.1$ (as conservative assumption). In this study Thevenin type arc model in EMTP-ATP programmed in MODELS language is preferred [7].

The dielectrical arc extinction phenomenon depends on various external factors around the free burning arc in air. Therefore, it cannot be modelled with certain accuracy and reliance. The arc extinction criterion in this study is based on thermal instability of arc described using conditions in (2). The arc extinguishes, if the time derivative of instantaneous arc resistance, dr'/dt, exceeds a pre-defined limit provided arc conductance g' per length is less than a certain value. The following limiting values per arc length are determined empirically:

$$g'_{\min} = 50\,\mu\mathrm{S}\cdot\mathrm{m};\ \frac{dr'}{dt} = 20\,\mathrm{M\Omega}/(\mathrm{s}\cdot\mathrm{m}) \tag{2}$$

During interruption of the faulty phase with the arc fault, a voltage from the sound phases of the double-circuit OHL is coupled to the faulty phase by capacitive and inductive coupling.

As the arc elongates the arc voltage increases with the arc length. When the arc voltage is in the range of the voltage coupled by the sound phases without arc, the arc becomes unstable. Therefore, it is important to determine the steady-state coupled voltage to the concerning phase disconnected at both ends without fault. The arc elongation speed is also very important to determine the secondary arc duration. In order to obtain the maximum arc duration, the elongation speed is assumed to be significantly low [8], i. e. the secondary arc reaches 10 times of its original length in 1 s. In reality, it may happen that the recovery voltage makes the high resistance arc channel zones reignite during arc elongation period. If the recovery voltage is sufficient to produce a breakdown, bridging a significant length of the arc channel occurs, the arcing process may return to the steady-state condition, remarkably prolonging the self-extinction time. In this analysis, the likely dielectrical breakdowns within the arc channel are not considered.

III. Studied Cases and Results

A. Overview

The main objective of this investigation is to estimate the maximum secondary arc duration for a SPAR operation on this mixed line. It is desired that the dead time should remain below 1 s in the worst case. In order to obtain a statement as reliable as possible, various factors were taken into account, which are described below.

- Operating current of the double-circuit line prior to the fault: 2800 A in each circuit; 4000 A in one circuit, the second circuit is out of service; both circuits at no load (far end is open) with the source voltage 410 kV at the sending end.
- Operating voltage of the line is set to the highest voltage for equipment $(U_m = 420\ \mathrm{kV})$ for the voltage source of the Thevenin equivalent of the source networks in substations S/S A and S/S D, when the line transmits power.
- Switching status of the second circuit of the 380-kV double-circuit line: both circuits or only one circuit in operation.
- Number of shunt reactors in the S/S A and D is varied, no shunt reactor, one or two shunt reactors are in operation.
- Reversal of power flow on the line, either from S/S A to S/S D or vice versa. Influence of the short parallel external line due to the power flow in that line.

As mentioned in section II-E the steady-state recovery voltage (SSRV) U_{lg} (see Fig. 6) coupled to the interrupted "faulty" phase without any arc fault – this situation is equivalent to the state, when the secondary arc has already extinguished – is a determining characteristic for the secondary arc duration

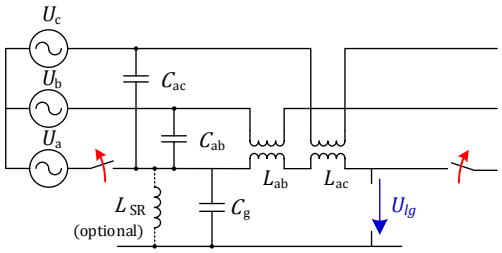

Fig. 6. State-state recovery voltage U_{lg} at fault location without arc influence

provided the arc elongation is linear [1]. Later in this paper, the strong correlation between the SSRV and the secondary arc duration, which will be determined by the simulation of electromagnetic transients, will be shown.

There is almost no impact of the shunt reactors on the secondary arc during single-phase interruption because they are not on the line side and do not influence the voltage coupled to the faulty phase as the opposite case illustrated in [1]. In Section III.D the influence of modifications in the system configuration on the secondary arc duration will be shown for a selected case.

B. Steady-state Recovery Voltage Analysis

As explained in the last section the SSRV has been computed by means of steady-state simulations for a variety of locations F1 to F5 along the transmission line as indicated in Fig. 7.

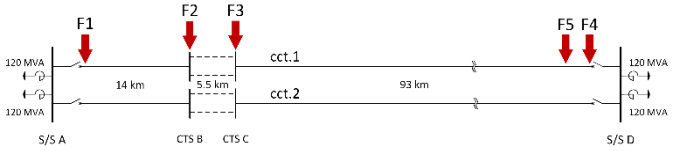

Fig. 7. Imaginary single-line-to-ground fault locations for SSRV analysis

The locations F1 and F4 are the sending and receiving end of the line behind the circuit breaker. F5 is 4 km away from F4. F2 and F3 point to the cable transfer stations.

Several cases with different pre-fault conditions and line configurations have been analyzed taking various factors mentioned in this section into consideration. The pre-fault operating conditions for the cases are defined in Table III and the computations of SSRV associated with those cases are summarized in Table IV.

TABLE III
PRE-FAULT OPERATING CONDITIONS

Config.	Description
A1	both circuits are in operation with 2800 A in each circuit; power flow direction from S/S A to S/S D
A2	both circuits are in operation with 2800 A in each circuit; power flow direction from S/S D to S/S A
B0	both circuits are at no load; energization from S/S A, CBs of both circuits at S/S D are open.
C1	circuit 1 is at no load; energization from S/S A; CB at S/S D is open; circuit 2 is switched off
C2	circuit 2 is at no load; energization from S/S A; CB at S/S D is open; circuit 1 is switched off
D1	circuit 1 is in operation with 4000 A; power flow direction from S/S A to S/S D; circuit 2 is switched off
D2	circuit 1 is in operation with 4000 A; power flow direction from S/S D to S/S A; circuit 2 is switched off
E1	circuit 2 is in operation with 4000 A; power flow direction from S/S A to S/S D; circuit 1 is switched off
E2	circuit 2 is in operation with 4000 A; power flow direction from S/S D to S/S A; circuit 1 is switched off

TABLE IV
MAXIMUM STEADY-STATE RECOVERY VOLTAGES AND THEIR LOCATION EXPECTED FOR EACH CONFIGURATION

case no.	config.	circuit	disconnected phase	location of max. U_{lg}	SSRV U_{lg} (kV)
1	A1	1	B	F4	20.5
2	A1	2	B	F4	19.4
3	A2	1	C	F4	**21.5**
4	A2	2	C	F4	**21.5**
5	B0	1	C	F2	18.5
6	B0	2	C	F2/F3	17.8
7	C1	1	C	F2/F3	19.2
8	C2	2	B	F2	18.7
9	D1	1	C	F4	29.7
10	D2	1	C	F4	**32.5**
11	E1	2	A	F4	29.5
12	E2	2	C	F4	31.6

According to Table IV the highest value of SSRV as RMS in case of operation of both circuits is 21.5 kV, whereas the maximum value of 32.5 kV is expected in case #10, if only one circuit is in operation with 4000 A line current and the second circuit is switched off. Consequently, the secondary arc duration is supposed to be longest for the case no. 10.

C. EMTP Simulations of the SPAR for various Cases

For the selected cases from Table IV EMTP-ATP simulations of the single-phase arc fault and the subsequent disconnection of the faulty phase with the arc model have been performed and the secondary arc duration has been determined. It is the elapsed time from the instance of circuit breaker pole opening at both ends of the faulty phase until the arc extinction. The SSRV and secondary arc duration are compared for the selected cases in the same diagram as shown in Fig. 8.

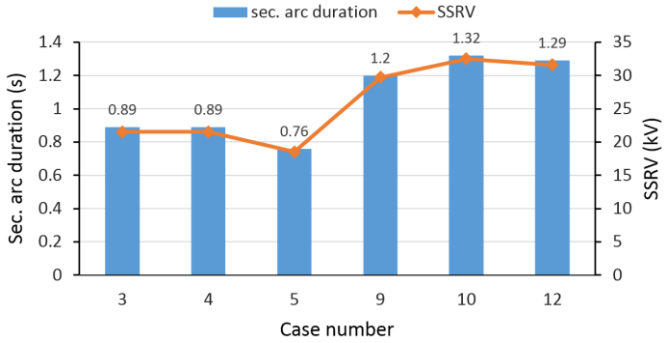

Fig. 8. Comparison of the SSRV with the secondary arc duration for the selected cases from Table IV

Obviously, there is a strong correlation between SSRV and the secondary arc duration (correlation coeff.: 0.99964), provided the elongation speed of the secondary arc is constant and there are no local breakdowns in the arc channel while the arc steadily stretches. This observation is generally in line with the results presented in [13]. However, a dependence of the arc duration on the ideal secondary arc current (without arc interaction) is not verifiable. The maximum arc duration is determined by means of a simulation as 1.32 s for the case no. 10. For the cases 3 and 4, where SPAR is applied as both 380-kV circuits are operation with a line current of 2800 A (config. A2), the arc duration is 0.89 s and shorter than 1 s. For the configuration A2 the dependency of the SSRV on the fault location has been studied. In circuit 1 the SSRV for the

disconnected phase *C* at all locations F1 to F5 has been computed and in the second step the secondary arc duration for those fault locations has been determined by means of simulations. The results of this analysis are shown in Fig. 9. The slow increase of the SSRV and the secondary arc duration at fault locations F1 to F5 along the line from S/S A toward S/S D depends on the voltage increase in sound phases of both circuits along the line due to power flow and different short-circuit impedances of the source networks at substations A and D.

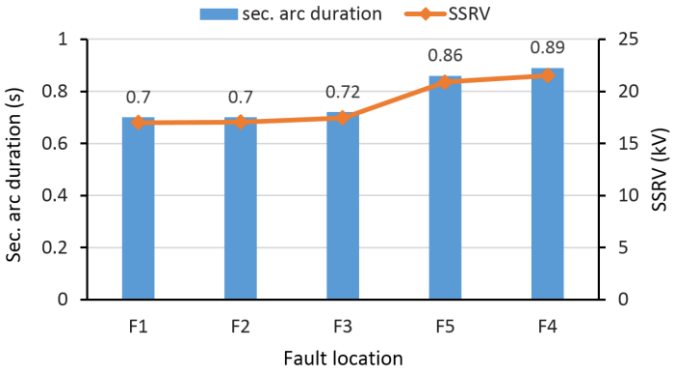

Fig. 9. SSRV and secondary arc duration for the configuration A2 at different fault locations along the 380-kV line (correlation coeff.: 0.99973)

The influence of the parallel 110-kV lines on the same tower on SSRV and on the secondary arc duration is negligible. Similarly, the influence of the external 380-kV double-circuit line (4.6 km parallel routing on the same tower) is also insignificant, i. e. SSRV deviation is smaller than 1.3 % for the power flow reversal on that external line.

In general, the secondary arc duration is longer for the configurations of only one 380-kV circuit is in operation with a higher line current. Due to the asymmetry of the OHL line sections with regard to the cable section (see Fig. 1) and different short-circuit impedances of the source networks at the S/S A and S/S D, the secondary arc duration tends to be greater as the single-line-to-ground fault is nearer to S/S D.

The voltage coupled to the faulty phase (SSRV) is also dependent on the position of phase conductors on the tower along the line. Since the double-circuit 380-kV line is transposed several times – not shown in the single-line diagram – it is difficult to identify the phase conductors with higher SSRV analytically. According to Table IV phase *C* of both circuits as the faulty phase tends to cause higher SSRV and secondary arc duration.

For the case no. 10 with the single-line-to ground arc fault in phase *C* at location F4 the results of the SPAR for certain quantities will be shown, where the fault arc is represented by the dynamical arc model (see section II.E). The currents of the circuit breakers (CB) at the S/S A and S/S D are shown in Fig. 10 and Fig. 11, respectively. The time window shows the incidence of the fault at voltage peak (see Fig. 12) and the opening of the CB pole C at $t = 0.1$ s at both line ends. From this moment on the secondary arc is active. Assuming the line-to-ground fault occurs at the last tower, an additional constant footing resistance of 1 Ω is used in series with the fault arc. The current of the CB pole *C* at S/S A remains almost unchanged as the fault is initiated at the far end of the line.

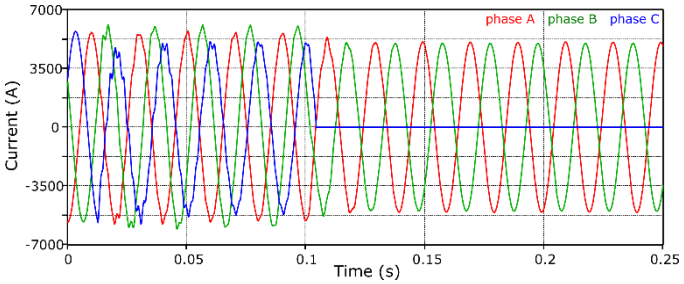

Fig. 10. Current of the CB at S/S A

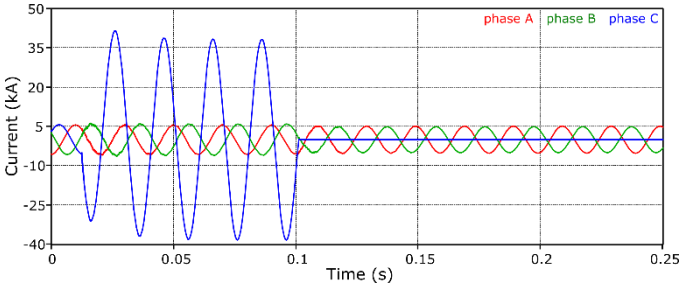

Fig. 11. Current of the CB at S/S D

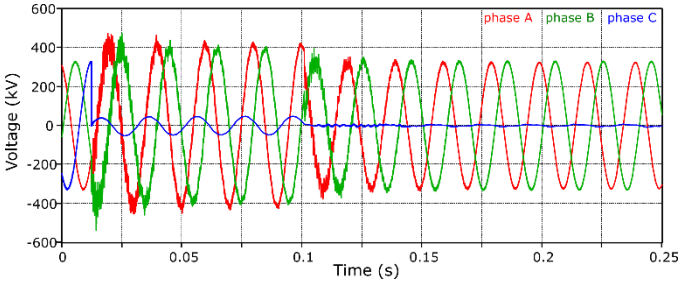

Fig. 12. Phase-to-ground voltages at fault location F4

The equivalent series branch between S/S A and S/S D (see Table I) representing surrounding lines is an additional path for the short-circuit current. Besides, the short-circuit impedance at S/S A is significantly greater than at S/S D.

The voltage and current of the fault arc are shown in Fig. 13. In the diagram there is also a mark of the arc extinction. As the arc elongates the arc voltage increases, which reaches and exceeds roughly the voltage level of $\sqrt{2} \cdot SSRV = 46$ kV and becomes unstable. In order to obtain the worst case for the secondary arc duration, the arc elongation is assumed to be as slow as possible [8], [9].

It is interesting to compare the fault arc behavior, when the fault is at a different place along the line. For comparison, the single-line-to-ground fault at F2 – very near to CTS C of the underground cable section – is taken into consideration with a subsequent single-phase interruption of the same faulty phase *C*

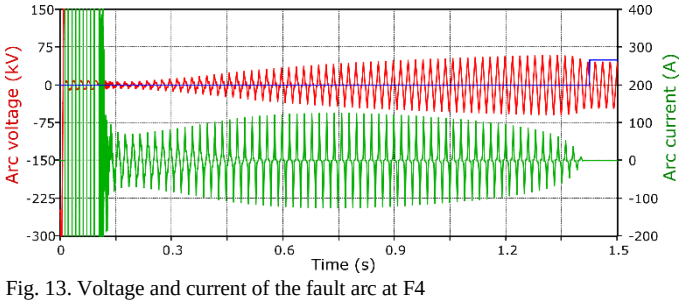

Fig. 13. Voltage and current of the fault arc at F4

by the CB's at the substations A and D. The currents of the CB's at S/S A and S/S D are shown in Fig. 14 and Fig. 15, respectively.

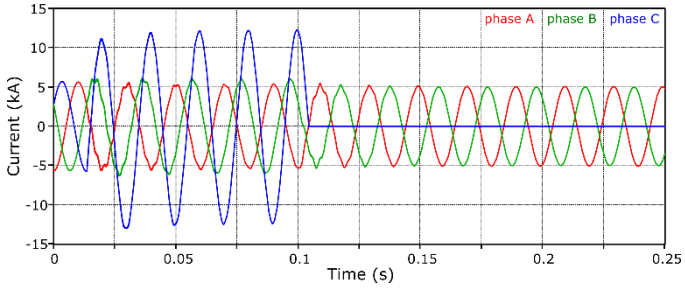

Fig. 14. Current of the CB at S/S A for the arc fault at F2

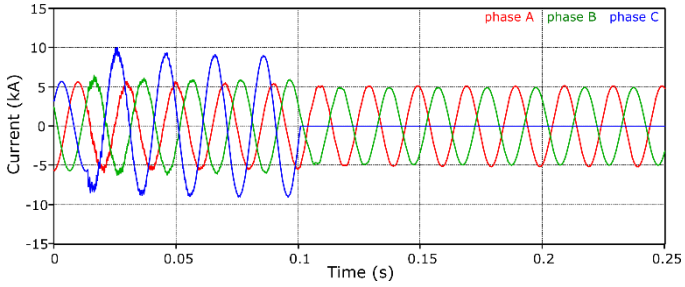

Fig. 15. Current of the CB at S/S D for the arc fault at F2

At this fault location the fault current is supplied from both ends of the line. The arc voltage for both fault locations F2 and F4 is compared in Fig. 16.

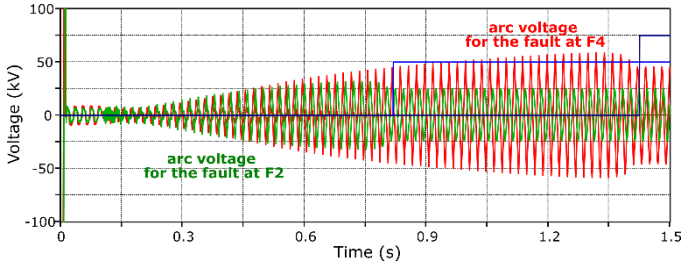

Fig. 16. Comparison of the arc voltage at the fault locations F2 and F4

Since the SSRV at fault location F2 with a value of 17.7 kV is much smaller than 32.5 kV at F4, the arc extinguishes earlier. The secondary arc duration 0.72 s is much shorter than 1.32 s. The analysis of the RMS value of the arc current supports also the fact that the energy of the arc column for the fault at F2 is less than for a fault at F4 as compared in Fig. 17.

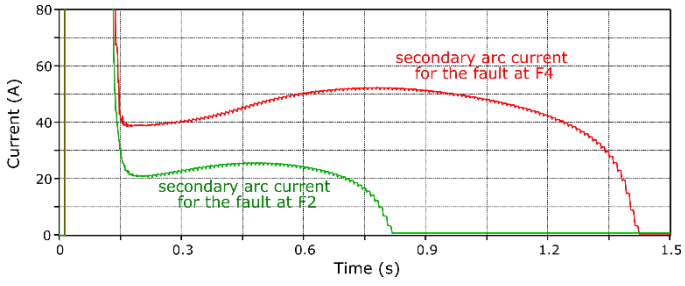

Fig. 17. RMS curves of the secondary arc current for the single-line-to-ground faults at F2 and F4

At the time point t = 0.15 s the secondary arc phase starts with different arc currents (F2: 20 A vs. F4: 40 A) and continues approximately with the same current ratio up to arc extinction. The arc voltage for both fault cases has in the interval from 0.15 s up to ca. 0.5 s almost the same time response. Consequently, the fault arc at F2 extinguishes earlier compared to the fault arc at F4, which is more sustainable due to higher coupled voltage and arc current.

D. Influence of the Structural Changes on the Secondary Arc Duration

The main factor influencing the secondary arc duration is SSRV, which again is dependent on the line configuration (length of the cable section relative to the total line length), OHL transpositions and line loading. Another important factor is the location of the shunt reactors. In this paper, the shunt reactors are located in the substations as a result of the operational policy of the TSO. Also, the cable section length is selected according to the environmental conditions. At this point, it would be interesting to understand the influence of the structural changes on the secondary arc extinction, i.e. secondary arc duration. In this regard, following structural variations on the transmission line are considered for the configuration D2 (refer to Table III) that causes the longest secondary arc duration:

D2a. Cable section is replaced by an OHL of the same length (5.5 km); shunt reactors remain connected to the S/S A and D.

D2b. Two shunt reactors (120 MVA each) are placed on the terminals CTS B and C of the cable section of circuit 1 (see Fig. 1).

D2c. Original configuration D2 remains unchanged; the elongation speed of the arc length will be increased by 150 % referring to the selected rather low speed [8] that is 29.4 m/s (the secondary arc will reach 10 times its initial length (3 m) within 1 s).

D2d. Original configuration D2 remains unchanged; the pre-fault line current will be reduced to 2 kA.

Since the cable section with a relatively high capacitance $C_{coaxial}$ that contributes to the line-to-ground capacitance C_g in Fig. 6 will be replaced by an OHL section that contributes to the mutual capacitance C_{ab} and C_{ac} (Fig. 6), and at the same time C_g will become less, the SSRV (U_{lg}) along the disconnected phase will be higher in case D2a compared to the original configuration D2 based on the capacitive voltage divider principle.. In case D2b, shunt reactors with the rated power 120 MVA as an inductive component will compensate 56 % of the capacitive charging current of the cable and OHL sections, the magnitude of the impedance of the parallel circuit consisting of L_{SR} and C_g will increase causing SSRV to become higher compared to the original configuration D2. Hence a longer arc duration is to be expected in cases D2a and D2b. In cases D2c and D2d the arc duration should be shorter as it can be anticipated.

In that selected line configuration D2 with the longest arc duration only the circuit 1 is in operation and the pre-fault line current is 4 kA. The faulty phase is *C*, where SPAR is applied. The results of the SSRV computation and the secondary arc duration determined by EMTP simulations are summarized in Table V.

TABLE V
SECONDARY ARC DURATION AND SSRV FOR THE STRUCTURAL VARIATIONS OF THE CONFIGURATION D2

Case	SSRV (kV) at F4, phase C	secondary arc duration (s)
D2 (original)	32.5	1.32
D2a	57.5	2.26
D2b	94.4	3.20
D2c	32.5	0.93
D2d	23.5	0.97

These case variations help to understand the interaction of the secondary arc with the surrounding transmission system during SPAR. An important parameter is the arc elongation speed which is independent of the SSRV at the fault location (case D2c). Again, the correlation between SSRV and the secondary arc duration is very high except case D2c, where the arc behavior is different. The correlation coefficient amounts to 0.9946 based on the data in Table V (without case D2c).

Based on the computations for this particular double-circuit 380-kV transmission line the secondary arc duration will be long, when only one circuit with a higher line current is in operation. For the configurations D and E in Table III, the reduction of the line current from 4 kA to 2 kA results in a shorter arc duration of less than 1 s as shown for the case D2d above. For the cases with relatively high secondary arc duration, adaptive autoreclosure with shorter dead time can be applied, provided the secondary arc will extinguish earlier due to the favorable external conditions like wind [10], [11]. Another method to shorten the secondary arc duration would be to install the so called four-legged reactors on the line side. However, their effectiveness for multi-circuit, multi-voltage transmission lines is rather low, more complex reactor schemes are necessary [15] and they are not preferred by the TSO's in Germany.

IV. CONCLUSIONS

The operation of the so called mixed EHV lines consisting of both overhead line and cable sections is relatively new and there exists less operational experience. In this regard certain aspects like the impact of such cable sections on the SPAR operation should be studied in advance by means of digital simulations. It is of vital importance to estimate the dead time required for the extinction of the secondary arc in case of single-line-to-ground fault in order to have a successful SPAR. For this purpose, the secondary arc duration under unfavorable conditions, i.e. with slow arc elongation speed, is determined by means of EMT simulations.

A realistic arc model has been used for the SPAR performance of the mixed EHV line, which has been developed and the arc parameters have been determined and optimized over the past years by evaluating numerous arc tests and measurements across real line insulators resulting in a very good agreement of measurements and simulations [4], [5], [6], [7].

The influence of various operational factors on the secondary arc duration has been studied. It has been shown that the steady-state recovery voltage at the fault location without fault is a reliable indicator for the duration of the secondary arc. The location of the shunt reactors in the substations, not on the line side, is a benefit with regard to the secondary arc duration because the SSRV of the faulty phase disconnected at both ends is in this case relatively low resulting in a shorter arc duration. The cable section integrated in the mixed EHV line has a positive influence on the secondary arc duration due to lower SSRV caused by the higher coaxial capacitance of the XLPE cable. Using the developed and verified model of an arc burning in air, the maximum secondary arc duration can be estimated by means of simulations under various operating conditions as a worst case scenario by selecting the arc parameters on the safe side. Those are the arc elongation speed and the change of arc time constant as a function of arc length.

V. REFERENCES

[1] M. Kizilcay, K. Teichmann, S. Papenheim und P. Malicki, "Analysis of Switching Transients of an EHV Transmission Line Consisting of Mixed Power Cable and Overhead Line Sections," in IPST - International Conf. on Power System Transients, Seoul, Korea, 2017. Available: https://www.ipstconf.org/Proc_IPST2017.php

[2] Canadian/American EMTP User Group *ATP Rule Book*, Portland, Oregon/USA, revised and distributed by the EEUG Association (http://www.eeug.org), last revision, 2017.

[3] H. K. Hoidalen, ATPDraw version 6.3 for Windows, 2015 – latest version available 7.3 – (https://www.atpdraw.net).

[4] M. Kizilcay, T. Pniok, "Digital Simulation of Fault Arcs in Power Systems", *ETEP Journal*, vol., 1, no. 1, pp. 55-60, 1991.

[5] M. Kizilcay, K.-H. Koch, "Numerical fault arc simulation based on power arc tests", *ETEP Journal*, vol. 4, no. 3, pp. 177-186, May/June 1994.

[6] M. Kizilcay, G. Bán, L. Prikler, P. Handl, "Interaction of the Secondary Arc with the Transmission System during Single-Phase Autoreclosure", in *Proc. 2003 IEEE Bologna Power Tech Conference*, Bologna, Italy.

[7] M. Kizilcay, P. La Seta, "Digital simulation of fault arcs in medium-voltage distribution networks", in *Proc. 2005 15th Power Systems Computation Conference*, Liège, Belgium.

[8] A.T. Johns, R.K. Aggarwal, Y.H. Song, 1994; "Improved Techniques for Modeling Fault Arcs on Faulted EHV Transmission System", *Proc. 1994 IEE - Generation, Transmission and Distribution*, vol. 141, no. 2, pp.148-154.

[9] M. Kizilcay, P. Malicki, S. Papenheim, M. Lösing, K. Vennemann, "Influence of shunt compensated EHV transmission lines consisting of several overhead line and XLPE cable sections on system performance", in *Proc. CIGRE Symposium Aalborg 2019*, paper no. 11, Available: https://e-cigre.org/publication/SYMP_AAL_2019-symposium-aalborg-2019.

[10] J. Blumschein, Y. Yelgin, A. Ludwig, "Adaptive Autoreclosure to Increase System Stability and Reduce Stress to Circuit Breakers", in *Proc. 70th Annual Conference for Protective Relay Engineers*, 03-06.04.2017, Texas A&M University, Texas, USA.

[11] Z. Radojevic, V. Terzija, G. Preston, S. Padmanabhan, D. Novosel, "Smart Overhead Lines Autoreclosure Algorithm Based on Detailed Fault Analysis", *IEEE Transactions on Smart Grid*, vol. 4, pp. 1829-1838, 2013.

[12] E. Haginomori, T. Koshiduka, J. Arai, H. Ikeda, *Power System Transient Analysis*, John Wiley & Sons, Ltd., United Kingdom, 2016.

[13] F. Gatta, A. Geri, M. Graziani, S. Lauria, M. Maccioni, "Single-pole autoreclosure in uncompensated EHV AC mixed overhead-cable lines: a parametric time-domain analysis", *Electric Power System Research*, vol. 210, Sept. 2022.

[14] F. Gatta, A. Geri, S. Lauria, M. Maccioni, "Power frequency secondary arc current in' uncompensated EHV AC mixed overhead-cable lines", *Electric Power System Research*, vol. 111, June 2014.

[15] J. S. Acosta, M. C. Tavares, A. M. Gole, "Neutral Reactor Structures for Improved Single Phase Auto Reclosing in Multi-Circuit Multi-Voltage Transmission Lines", IEEE Trans. on Power Delivery, vol. 37, pp. 298-307, Feb. 2022.